Thermal, dielectric and electrochemical study of decanoic acidtetrabutylammonium chloride deep eutectic solvent Étude thermique, diélectrique et électrochimique du solvant eutectique profond acide décanoïquechlorure de tetrabutylammonium

Mohammad Nadim Kamar, Ludovic Paquin, Emmanuelle Limanton, Corinne Lagrost, Denis Morineau

Thermal, dielectric and electrochemical study of decanoic acid - tetrabutylammonium chloride deep eutectic solvent

Étude thermique, diélectrique et électrochimique du solvant eutectique profond acide décanoïque – chlorure de tetrabutylammonium

Mohammad Nadim Kamar[a], Ludovic Paquin[b], Emmanuelle Limanton[b], Corinne Lagrost[b], Denis Morineau[a]

[a]Institut de Physique de Rennes, CNRS-Université de Rennes, UMR 6251, F-35042 Rennes, France

[b]Institut des Sciences Chimiques de Rennes, CNRS-Université de Rennes, UMR 6226, F-35042 Rennes, France

Keywords: Deep Eutectic Solvents, Dielectric Spectroscopy, Electrochemistry

Mots-clés : Solvants Eutectiques Profonds, Spectroscopie Diélectrique, Électrochimie

Graphical abstract:

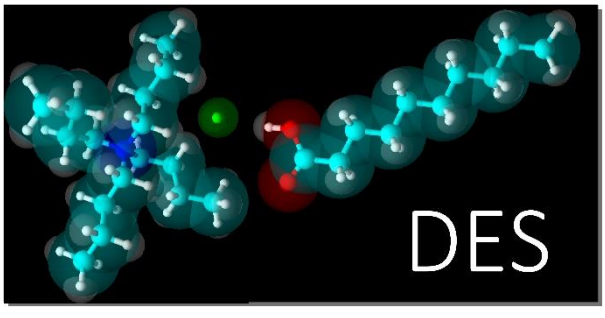

Abstract:

Mixture based on decanoic acid (DA) and tetrabutylammonium chloride (TBACl) is a simple and prototypical Deep Eutectic Solvent (DES) useful for extracting compounds that are poorly soluble in water or in electrochemical applications. The most widely studied molar composition is DA-TBACl molar ratio equal to (2:1). The composition of the DESs has a strong impact on their physicochemical properties. Herein a comparative study of the thermal, dielectric, ionic conductivity and electrochemical properties of DA-TBACl is carried out by varying the molar composition as (2:1), (1:1) and (1:2). All the molar compositions lead to stable fluid whose properties depend on the composition, bringing further insights in the fine understanding of the chemical interactions that prevail in those materials.

Corresponding Authors:

E-mail: denis.morineau@univ-rennes.fr, corinne.lagrost@univ-rennes.fr, ludovic.paquin@univ-rennes.fr

1. Introduction

Since pioneering studies in the early 2000s,[1] deep eutectic solvents (DESs) have developed as a new class of alternative solvents, complementing the potential offered by other unconventional media such as ionic liquids. They are promising in many applications,[2,3] notably as extracting media for natural compounds or for pesticides recovery or even for CO_2 capture to quote a few.[4–8]

Conservatively, DES is defined as a mixture of two or more H-bonded compounds that exhibits an eutectic point and large non-ideal mixing effects.[9] The non-ideal character of DES that relates to specific interactions between hydrogen bond donor (HBD) and hydrogen bond acceptor (HBA), significantly enhances the temperature depression of the melting point at the eutectic point. Interestingly, this effect has significantly expanded the number of candidates as ingredients for the formulation of these new solvents, as it allows the inclusion of compounds that are normally found in solid form at room temperature in their pure state. Beyond melting, non-ideality also implies that DESs present properties that differ from those of their constituents when considered independently, thus offering new opportunities to design solvents for specific applications.

The DESs have been classified into five classes, and notably the class III is of interest in this work where the HBA is an ionic constituent of an organic salt, typically a quaternary ammonium halide similarly to ionic liquids.[10] Type III systems have been then largely represented in the DESs panel, and are especially interesting for electrochemical applications. Most DESs proposed so far were of hydrophilic nature while increasing their hydrophobicity has become an important goal in order to expand their application scope.[11,12] For instance, higher hydrophobicity is interesting because it provides to DES the ability to dissolve natural products with limited water solubility like carotenoids for instance, also helping in the preservation of their antioxidant properties[7] and better performance in CO_2 capture.[8]

These characteristics are promoted by the combination of organic salts comprising long alkyl chains, with poorly water miscible HBD molecules, such as fatty acids. Since pioneering study in 2015, such systems are now commonly classified as “hydrophobic DESs” due to the low water content and low ion leaching after mixing with water.[12]

They have generally higher viscosities than hydrophilic DESs and exhibit lower to very weak conductivities : few of them could be indeed used as electrolyte in electrochemistry, since the “hydrophobic DESs” often belong to the type V, that is composed solely of molecular substances.[13,14] Yet, for application in electrochemistry, the composition of “hydrophobic DESs” will necessarily involve an organic salt. However, the question arises about the evolution of the polarity and conductivity as a function of the molar composition and the temperature. Herein, we address this point by focusing on one of the first reported and since widely studied “hydrophobic DESs” consisting of a mixture of decanoic acid (DA) as HBD and tetrabutylammonium chloride (TBACl) as HBA (Figure 1). We present a systematic study of the thermal, dielectric, ionic conductivity and electrochemical properties of DA-TBACl mixture as a function of the molar composition for three compositions (1:2, 1:1, 2:1), in order to cover the range of interest related to previous studies, including the most widely studied one (2:1).[11,12] The mixing of the corresponding eutectic mixtures with large amount of water is also qualitatively investigated according to the molar ratio of the eutectic components. The results show the strong impact of the hydrophobic DA component with respect to the ammonium salt to design a stable solvent of low polarity having good conductivity, reasonable viscosity and good electrochemical property.

2. Materials and methods

The decanoic acid (DA)- tetrabutylammonium chloride (TBACl) liquid mixtures were prepared for three different compositions, later denoted DA-TBACl (*n*:*m*), with *n*:*m* corresponding to the molar stoichiometry. DA and TBACl were purchased from Acros Organics and were used

without further purification. DA (melting point 31.5 °C) and TBACl (melting point 83-86°C) were mixed in molar ratio 1:1, 2:1 and 1:2 at 80°C under stirring for 2 h until a homogeneous and transparent liquid was obtained. Then, the mixtures were allowed to cool at room temperature and stored under ambient conditions. The colorless fluids are visually stable over time (more than 1 year). The water content of the resulting mixtures was determined by Karl-Fisher titration (831 KF Coulometer with a generator electrode with diaphragm, Metrohm) with an average of three measurements. DA-TBACl (1:1) has 2.8% of water (w/w). DA-TBACl (2:1) has 1.7 % of water (w/w). DA-TBACl (1:2) has 3.4% of water (w/w)

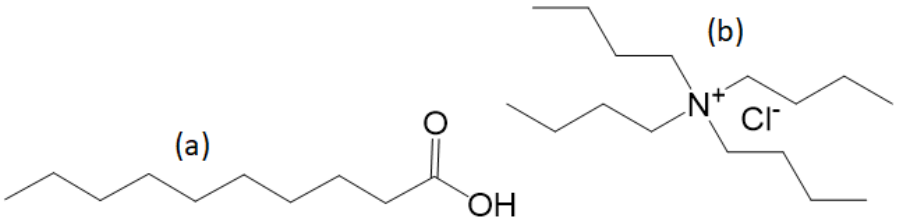

Figure 1. Chemical structure of (a) decanoic acid (DA) and (b) tetrabutylammonium chloride (TBACl)**.**

For differential scanning calorimetry (DSC) experiments, the weighted samples were sealed in Tzero© aluminum hermetic pans. The measurements were performed with a Q-20 TA instrument equipped with a liquid nitrogen cooling system. The standard calibration of temperature and heat flux was performed by measuring the melting transition of an indium sample. The thermograms were acquired on cooling, followed by a heating ramp in the temperature range from -120 to 35 °C with the same scanning rate of 5 °C.min^{-1}. For DA-TBACl (2:1), an additional measurement of the heating ramp at 5 °C.min^{-1} was performed after a fast thermal quench at maximum cooling rate (ca. 200 °C. min^{-1}) to avoid crystallization (see discussion for details).

For dielectric spectroscopy experiments, the samples were injected with a pipette between two stainless steel electrodes maintained by Teflon spacers, in order to form a parallel plate capacitor geometry with a diameter of 20 mm and a spacing of 260 μm. During this operation, both the liquids and the sample cell were heated up to about 60 °C to decrease viscosity and insure the fast and complete filling of the cell by the action of capillary forces. Then, the cell was placed in the cryostat and maintained under a dry nitrogen atmosphere. The complex impedance of the as-prepared capacitor was measured from 1 Hz to 10^6 Hz with a Novocontrol high resolution dielectric Alpha analyzer with an active sample cell. The measurements were performed at thermal equilibrium along a cooling branch and a subsequent heating branch with a temperature step of 2 °C, and typically covering the temperature range from (-120 °C to 60 °C). The temperature of the samples was controlled by a Quatro temperature controller (Novocontrol) with nitrogen as a heating/cooling agent providing a temperature stability within 0.1 °C. The temperature scan rate, although discontinuous, was about 0.3 °C.min^{-1} on average.

For electrochemical experiments, the measurements were performed by using a home-made three-electrode cell.[15] A glassy carbon disk electrode (Ø 1mm), a platinum wire and a silver wire were used as working, counter and quasi-reference electrodes, respectively. The working electrode was carefully polished with SiC paper and diamond paste (Struers), then rinsed with ultrapure water and dried with an argon flow prior to experiments. Cyclic voltammetry was carried out with an Autolab PGSTAT 30 potentiostat/galvanostat (Metrohm Autolab B.V.).

3. Results and discussion

3.1 Differential scanning calorimetry

The phase behavior of the three different samples was determined by differential scanning calorimetry. For the three systems, the same thermal cycling was first applied. It consists in cooling from 35 °C to -120 °C and heating up to 35 °C at 5 °C.min^{-1}. For DA-TBACl (1:2) and

DA-TBACl (1:1), no crystallization was observed, neither on cooling nor on heating as presented in supplementary information (Figures S1 and S2). This means that for these compositions, DA-TBACl mixtures can be easily supercooled and form very good glassforming systems. Indeed, a glass transition was clearly demonstrated by a jump in the heat capacity. In contrast for DA-TBACl (2:1), crystallization occurred during cooling, as indicated by an exothermic peak in Figure S3. This crystallization concerned only a fraction of the sample. In fact, the remaining liquid phase performed a glass transition and eventually fully crystallized during the subsequent heating (Figure S3). In order to form a glass that was free from partial crystallization, the DA-TBACl (2:1) system was quenched by cooling at maximum rate (200 °C.min^{-1}). Under these conditions, the absence of exothermic signal during cooling indicated the successful formation of a pure amorphous glassy state.

On heating above the glass transition temperature T_g, the supercooled liquid of DA-TBACl (2:1) crystallized at -55 °C (cold crystallization) and then melted on a broad temperature with two main endothermic peaks centered at -25 °C and -10 °C. These features are characteristics of the melting of eutectic forming binary systems at a composition that differs from the eutectic point.[16] On the other hand, it has been shown that DES exhibits a better glassforming tendency for compositions neighboring the eutectic one, as seen for the two other DA-TBACl systems. The precise determination of the eutectic point, though interesting, would require a systematic study of the entire phase diagram, which lies out of the scope of the present study dedicated to the liquid phase properties. Moreover, due to its very good glass-forming capability on a broad range on composition, the precise determination of the eutectic point would probably be elusive.

In order to focus on the longtime liquid dynamics, the glass transition of the three samples is compared in Figure 2. On increasing the relative amount of the organic salt (TBACl) in the mixture, the position of the heat capacity jump systematically shifted to higher temperature, with the glass transition temperatures being respectively Tg = -83.8°C, -76°C, and -63.1°C.

This means that, for this range of compositions, the relaxation dynamics of the mixture slow down by adding TBACl to DA. This is in agreement with the observed increase of viscosity of the solvents at room temperature.

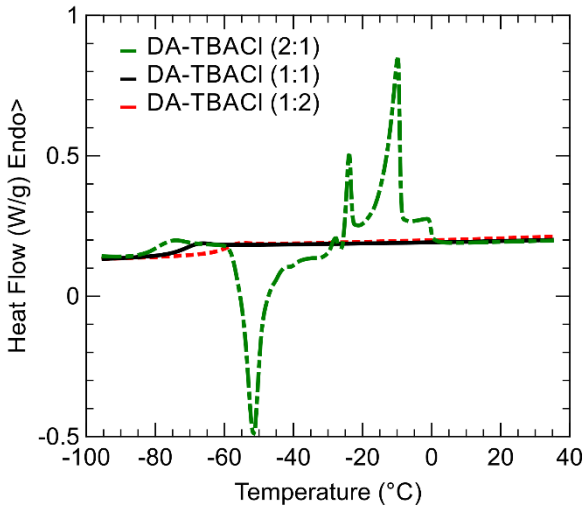

Figure 2. Thermograms measured during heating at 5°C.min^{-1} of DA-TBACl mixtures with composition (green dashed-dotted) 2:1, (solid black) 1:1, and (dashed red) 1:2. These heating ramps were acquired after cooling at the same rate, except for DA-TBACl (2:1) where a thermal quench was applied.

This dependence of T_g on the composition can be interpreted as resulting from an increase of intermolecular correlations between the different species of the mixtures due to enhanced H-bonds and electrostatic interactions between DA and TBACl. Such interactions are often invoked in DESs and also related to unusual thermodynamic or structural features, such as the formation of supramolecular species.[17–22] However, it is worth pointing out that mixing effects on the dynamical properties of DESs are not systematically observed. For instance, opposite effects of adding choline chloride into neat polyols have been reported for glyceline and for ethaline, respectively.[23] As a whole, the different dependences of the glassy dynamics on the composition of the liquid mixture illustrate the complexity of intermolecular correlations in

DESs that result from the balance between H-bonds, electrostatic interactions and, herein, hydrophobic interactions.

The calorimetric glass transition offers a limited view of the DES dynamics, typically restricted to relaxation timescale of the order of 10^2 s. This corresponds to temperature at which the system is extremely viscous. In order to link the glass transition to the actual dynamics in the fluid liquid state, a complementary study by spectroscopic methods is valuable.

3.2 Dielectric spectroscopy

Dielectric spectroscopy has been demonstrated to be a very powerful method for DESs studies.[16,23–25] It covers an extended dynamical range bridging the gap from molecular to calorimetric timescales, while providing insights into both the ionic transport (conductivity) and dipolar relaxation (polarization).

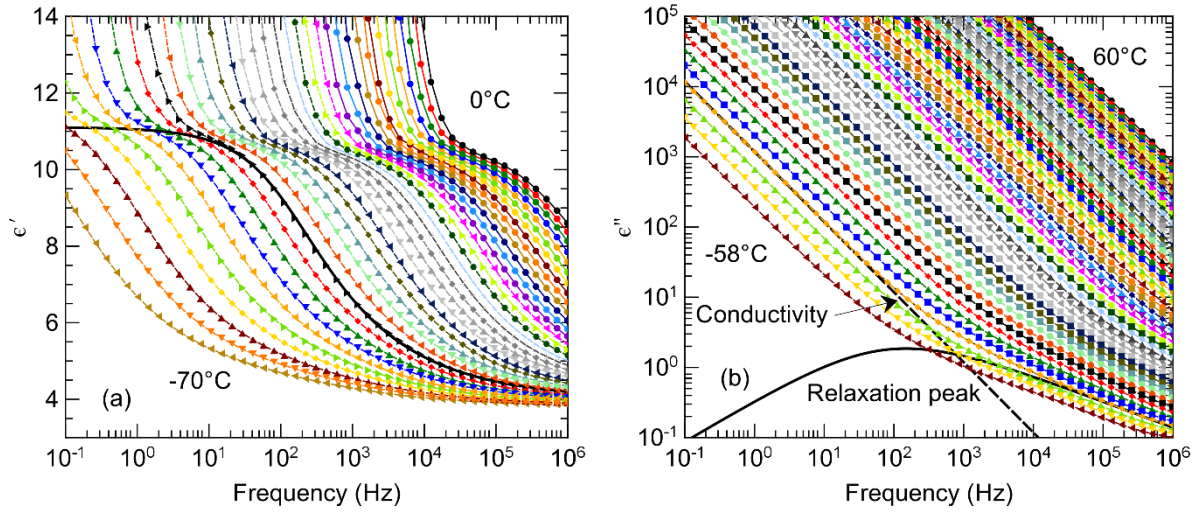

Figure 3. (a) real and (b) loss parts of the complex dielectric function of DA-TBACl (1:1) as a function of the frequency for a selection of temperatures regularly spaced by steps of 2 °C (the lowest and highest temperature values are indicated in each panel). The total fitted functions (thin dashed lines) are virtually indistinguishable from the experimental data points (symbols).

The individual contributions from dipolar relaxation (thick black solid line) and conductivity (thick dashed line) to the total fitted function are illustrated for the temperature *T*= -52°C.

The complex dielectric function of the sample $\varepsilon^*(f) = \varepsilon'(f) - i\varepsilon''(f)$ was measured for the three samples by cooling steps of 2 °C where *f* denotes the frequency of the electric field that ranges from 0.1Hz to 1MHz., ε' and ε'' the real and loss part of the complex dielectric function and *i* symbolizes the imaginary unit.[26] They are illustrated in Figure 3 for DA-TBACl (1:1) and for a selection of temperatures. Different contributions can be identified as a function of the frequency and the temperature. First, a considerable increase of the real part of the permittivity was observed at the high temperature and low frequency. This effect is classically attributed to electrode polarization induced by the accumulation of ions at the surface of the blocking electrodes.[26] This phenomenon does not bring any useful physically information about the liquid properties, and its contribution to the total intensity could be simply accounted by a phenomenological power law function.

The most remarkable observed feature is the prominent dipolar relaxation process that is illustrated in Figure 3a by the jump of ε'(*f*) from static permittivity ε_s to high-frequency permittivity ε_∞. This relaxation process is also apparent in the loss part ε''(*f*) although its corresponding peak (see dashed line in Figure 3b) is overwhelmed by conductivity that additionally contributes to ε''(*f*).

The dielectric relaxation and the ionic conductivity were analyzed quantitatively at each temperature by fitting a model comprising a Havriliak and Negami functions (HN-model),[27] and a dc-conductivity term according to eq. 1

$$\varepsilon^*(\omega) = \varepsilon_\infty + \frac{\Delta\varepsilon}{(1+(i\omega\tau_{HN})^{\alpha_{HN}})^{\beta_{HN}}} - i\frac{\sigma}{\omega\varepsilon_0} \qquad (1)$$

In this model, $\omega = 2\pi f$, ε_∞ is the sample permittivity in the limit of high frequency, $\Delta\varepsilon = \varepsilon_s - \varepsilon_\infty$ and τ_{HN} are respectively the dielectric strength and the HN-relaxation time of the mode. σ stands for the dc-conductivity of the sample and ε_0 the permittivity of vacuum. According to the formalism of the HN-model, the exponents α_{HN} and β_{HN} ($0 < \alpha_{HN}$; $\alpha_{HN}\beta_{HN} \leq 1$) are fractional parameters describing, respectively, the symmetric and asymmetric broadening of the complex dielectric function with respect to the Debye one.

First, we consider the static dielectric permittivity ε_s, which is an important indicator of the polar character of solvents. For DA-TBACl (2:1), we found $\varepsilon_s = 6.5 \pm 0.5$, with negligible temperature effects in the range studied, while larger values were found for the two other compositions i.e., $\varepsilon_s = 11 \pm 1$. The increase of ε_s with the addition of TBACl when going from (2:1) to (1:1) is most probably associated to the large polar character of the ionic component TBACl. However, the saturation of ε_s with salt content when further increasing the fraction of TBACl from (1:1) to (1:2) demonstrates that, not only the individual dipoles of species in the mixture, but also their relative spatial arrangement determines the dielectric permittivity of the solvent. Indeed, the Kirkwood−Fröhlich formalism accounts for the role of angular correlations between the dipoles of different molecules present in liquid. In this framework, the evolution of ε_s among the three samples would be consistent with the gradual formation of DA-TBACl supramolecular arrangements that promote the antiparallel dipolar configurations of TBACl ions.[28] This possibility definitely requests complementary structural characterizations, as accessible by optical spectroscopy or diffraction methods.

Beyond static information gained from ε_s, we discuss now the liquid dynamics. The average relaxation time, that is classically related to the maximum peak position in the lost part of the complex dielectric function was evaluated by eq. 2.[29]

$$\tau = \tau_{HN} \sin\left(\frac{\pi\alpha_{HN}}{2+2\beta_{HN}}\right)^{-1/\alpha_{HN}} \sin\left(\frac{\pi\alpha_{HN}\beta_{HN}}{2+2\beta_{HN}}\right)^{1/\alpha_{HN}} \quad (2)$$

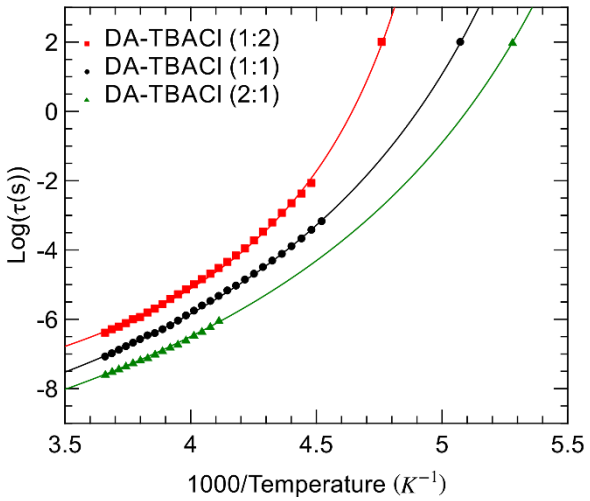

Figure 4. Arrhenius plot of the dipolar relaxation time of the studied DA-TBACl mixtures with composition (green triangles) 2:1, (black circles) 1:1, and (red squares) 1:2. The calorimetric glass transition is indicated by the symbol located at τ=10^2s. VTF fits are illustrated by solid lines.

The temperature dependence of the relaxation time is illustrated in Fig. 4 in Arrhenius coordinates. Note that for DA-TBACl (2:1) the accessible temperature range was reduced due to crystallization on cooling at about -36°C. Deviation from the Arrhenius law was observed for the three samples. This phenomenon is typical for supercooled liquids, and it has also been reported for many DESs.[16,23–25] It is often associated to the emergence of cooperativity that leads to an increase of the apparent activation energy on approaching the glass transition. Very good fits to the data were achieved with the Vogel–Fulcher–Tammann (VFT) law, as illustrated by solid line. The extrapolation of the relaxation time using the VFT law toward τ=10^2s

provides an estimate of the glass transition temperature that is in perfect agreement with the calorimetric one (see symbol in Fig. 3). This demonstrates that the dipolar relaxation measured by dielectric spectroscopy is directly coupled to the main structural relaxation of the liquid. A systematic slowdown of the relaxation dynamics is obtained when increasing the fraction of TBACl into the liquid mixture. This agrees with the conclusion made from the DSC part. In addition, we have used the VTF fits to compute the fragility index *m*, which is a measure of the deviation from the Arrhenian behavior.[30] The obtained values are in the range *m*=58-81, and increase with increasing the fraction of TBACl. They are located between values obtained for choline chloride-based DESs and their aqueous solutions (*m*=40-60),[23,24] which are classified as intermediate liquids, on the one hand, and hydrophobic DESs based on Menthol-Thymol mixtures (*m* =77-86) which are classified as fragile (i.e. showing larger deviation from the Arrhenius law), on the other hand.[16]

In addition to the temperature dependence of the average relaxation time, another important feature is the deviation of the dipolar relaxation function from a simple Debye process. This salient behavior can be expressed in time domain by a stretched exponential function $e^{-\left(\frac{t}{\tau}\right)^{\beta}}$ also denoted Kohlrausch-William-Watts (KWW) law. While simple Debye relaxation is recovered for β=1, a stretched relaxation process is obtained for lower values of the β exponent. We evaluated the value of β using the HN fractional exponents obtained from the fit in the frequency domain and the numerical ansatz $\beta = (\alpha_{HN}\beta_{HN})^{\frac{1}{1.23}}$.[31]

On the temperature range studied, the stretching exponent was β = 0.7±0.05 for DA-TBACl (2:1), which indicates relatively weak deviation from the Debye law. On the contrary, much lower values of the KWW exponent (β = 0.45±0.05) were found for the two other compositions having a larger fraction of ionic species i.e. (1:1) and (1:2). For glassforming liquids, the non-Debye relaxation behavior is often attributed to dynamic heterogeneity. For DESs, a possible

origin of dynamic heterogeneity stems from the association of the different components of the mixtures, which has been shown to result in the formation of mesoscopic domains.[20–22] In this context, the broader distribution of relaxation times can arise from molecules experiencing different local environments.

3.3 Ionic dc-conductivity

In complement to dipolar relaxation, dielectric spectroscopy experiments provide useful information about the liquid dynamics from the dc-conductivity. As shown in Fig. 3b, the conductivity of the DESs appears as an intense component of the loss part of the dielectric function which is inversely proportional to frequency,

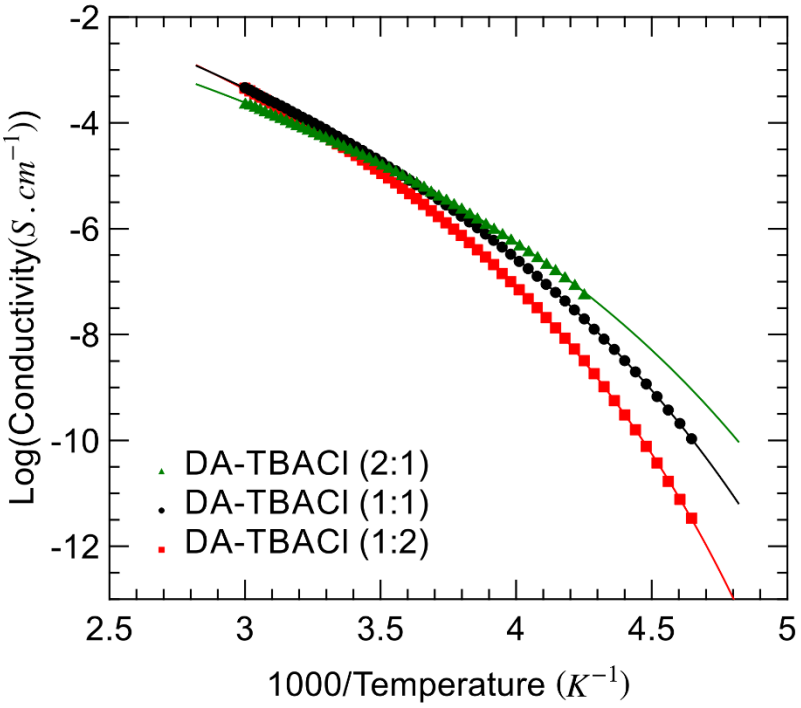

Figure 5. Arrhenius plot of the dc-conductivity of the studied DA-TBACl mixtures with composition (green triangles) 2:1, (black circles) 1:1, and (red squares) 1:2. VTF fits are illustrated by solid lines.

The temperature dependence of the conductivity, as determined by fitting of eq. 1, is illustrated in Fig. 5, in Arrhenius coordinates. For all samples, a super-Arrhenian behavior is obtained, which again could be well-reproduced by a VTF model. This temperature behavior is close to that of the dipolar relaxation, which suggests that both properties are actually linked. A possible explanation is that both processes reflect the temperature dependence of viscosity. On one hand, the dielectric relaxation relates in a large extent, to the rotational dynamics of dipolar species. Assuming the validity of classical hydrodynamics laws, the relaxation time should scale with the viscosity η according to the Stokes-Einstein-Debye equation $\tau \propto \frac{8\pi r \eta}{kT}$, with r being the hydrodynamic radius. On the second hand, the ionic conductivity should be inversely proportional to the viscosity, assuming that both the Nernst-Einstein and Stokes-Einstein relations apply. This predicted behavior was actually confirmed for DA-TBACl (2:1) and (1:1), as illustrated in Fig. S4. Contrariwise, this scaling law was only partly obeyed for DA-TBACl (1:2) that showed deviation in the high temperature limit.

In the literature, different situations have been recently reported about the (de-)coupling between rotation and translation dynamics in DESs. In the case of the prototypical ionic DES ethaline, no translation-rotation decoupling was observed neither for the neat mixture, nor for its moderately hydrated variants.[23–25] For the non-ionic menthol-thymol DES instead, a power law $\sigma \propto \tau^{-\alpha}$ was observed, with a fractional exponent α that was close to unity for equimolar composition, but increasingly deviated as the fraction of thymol in the mixture increased.[16] This partial decoupling was interpreted as a possible hint for the development of spatial dynamic heterogeneities in this range of compositions. Similarly, for reline, the deviation from the Walden rule that links ionic conductivity to viscosity was reported.[25] The presence of complex supramolecular structures was invoked as a possible origin of this unusual charge transport. Although based solely on dynamical properties, the observation made for DA-TBACl by

increasing the amount of salt also points toward the possible formation of supramolecular entities involving both ionic (TBACl) and H-bond donors (DA).

Finally, the inversion in the order of the conductivity values, which intersect approximately at room temperature, reflects the different impacts of TBACl on the liquid property. On the one hand, going from (2:1) to (1:2) DA-TBACl increases both the concentration of ionic mobile species and water content that contribute to high conductivity at high temperature. On the other hand, it increases the liquid fragility, which has negative impact on conductivity at sub-ambient temperature, since the viscosity increases more drastically on cooling with the TBACl stoichiometry.

3.3 Electrochemistry

The electrochemical behavior of the three mixtures is displayed in figure 6. The cyclic voltammetries (CV) have been recorded using a glassy carbon electrode with anodic and cathodic potential limits arbitrarily chosen. In agreement with the results above, all the mixtures are enough conducting to serve as electrolyte. The electrochemical window (i.e. the potentials range between the anodic and cathodic limits) is relatively shrinked compared to ionic liquids. The potential windows are about 2 V while ionic liquids show typical windows of 4.5-5 V.[32] This is probably due to the presence of water (2-3 wt %) and oxygen from air that accompanies water. However, the corresponding electrochemical windows are still larger than that of aqueous electrolytes.

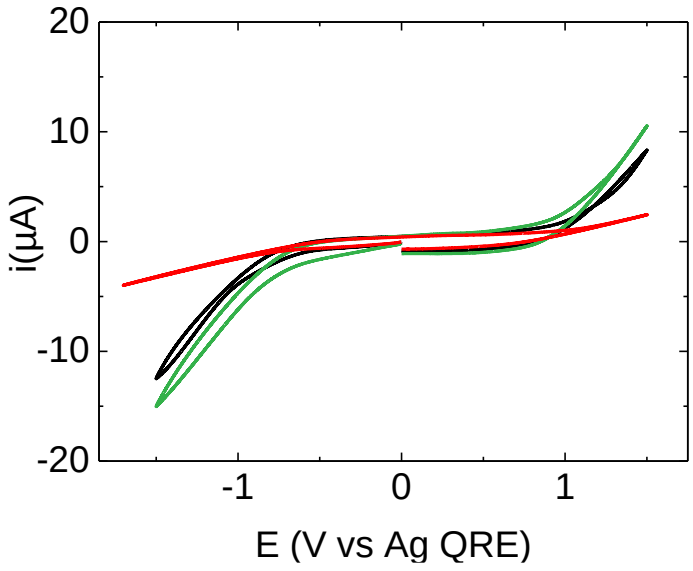

Figure 6. Cyclic voltammetries of the three DA-TBACl mixtures at 0.2 $V.s^{-1}$ at a glassy carbon disk electrode, (black) DA-TBACl (1:1), (green) DA-TBACl (2:1) and (red) DA-TBACl (1:2).

Another interesting point is the shape of the cyclic voltammetries which is different for DA-TBACl (1:1) and DA-TBACl (2:1) on the one hand and DA-TBACl (1:2) on the other hand. While DA-TBACl (1:1) and DA-TBACl (2:1) show a similar behaviour, the CV corresponding to DA-TBACl (1:2) is much more flattened than the two former ones, indicating a more resistive behaviour of DA-TBACl (1:2) than those of the two other compositions. This observation is in fair agreement with the ionic dc conductivity analyses.

3.4 Behaviour of the mixtures against water: qualitative examination

Hydrophobicity of the DES could be qualitatively assessed by the appearance of a phase separation after being mixed with a large amount of water. After vigorous stirring at ambient temperature, the three compositions tend to phase-separate (Figure 7) just after the mixing with 29 wt % of water. These behaviours are in good agreement with the dielectric measurements

above, suggesting that all the compositions give non-polar fluid. However, after three days, another equilibrium is reached and only the composition DA-TBACl (2:1) still exhibits a phase separation with water while the two other compositions are now mixed with water (Figure 7). Considering that TBACl is a hydrophilic component and DA a hydrophobic one, these observations show that the hydrophobicity character is obviously brought by DA, in molar excess for this mixture composition. Of course, leaching of the hydrophilic component could occur in the water-rich phase as already observed.[5] The clear mixing of hydrophobic DES with water is known to be sensitive to amount of water. For instance, the upper limit is found around 10 wt% for a DES formed with decanoic acid and tetrabutylammonium bromide (2:1).[8] A higher value of the water content upper limit is nevertheless found herein although that tetrabutylammonium bromide is less hydrophilic than its corresponding chloride counterpart. Interestingly, we also observe here that the water mixing is also strongly dependent on the molar ratio composition. A more precise microscopic description of the DES would be interesting to better understand the phenomena. However, we may rationalize the observations on the basis of hydrogen bonding effects since these interactions are of major importance for the preparation of these mixtures. Indeed in the DES, TBACl is likely to be hydrogen-bonded with DA to form a stable structure, even if a few amounts of water take part of the structure, probably also through the formation of hydrogen bonds between the eutectics and water. When increasing the water content, a competition may occur between the formation of hydrogen bonds of water with the HBD and HBA components of the eutectic mixture and the formation of hydrogen bonds between the two components that preserves the eutectic structure. At a certain point, and for large amount of water, the hydrogen bonds come mainly from water-"isolated" components association, hence destroying the fluid structure to enable an efficient mixing with water. In the case of choline chloride based DESs, a cross-over separating two distinct thermodynamic behaviors was observed for a water content of 30 wt%, from a "water-in-DES" to "DES-in-

water" situation, although no macroscopic liquid-liquid phase separation occurred at room temperature, due to their strong hydrophilic character compared to DA-TBACl.[33–35] Larger amount of HBD i.e. DA helps keeping the structure, even if the eutectic point is not necessarily reached. Hydrophobic eutectic mixtures can form stable mixing system with a certain molar fraction of water, depending on their own molar composition.

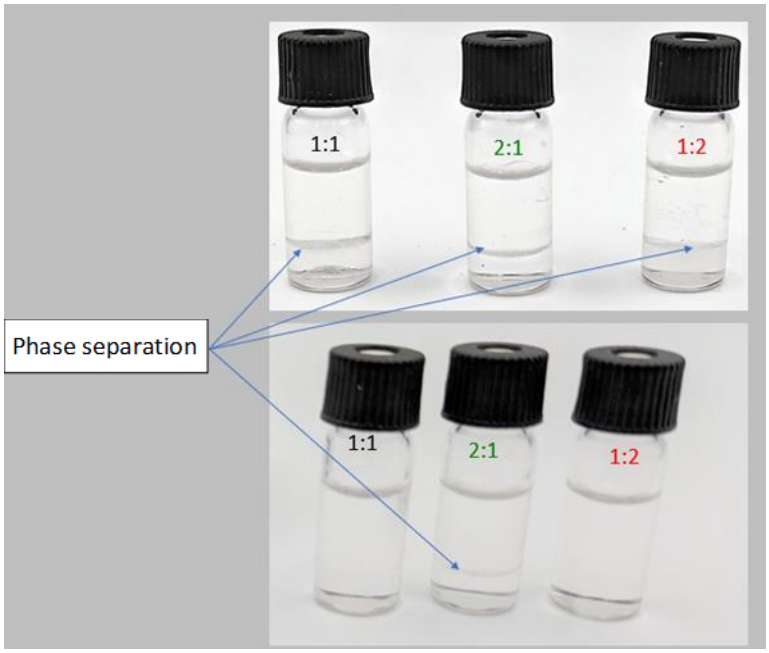

Figure 7. Pictures of 800 µL DA-TBACl (1:1), DA-TBACl (2:1) and DA-TBACl (1:2) just after mixing with 300 µL of water (top) and after three days (bottom)

4. Conclusion

In the quest of new solvents with designed properties, hydrophobic DESs are promising candidates to meet the important needs for extracting compounds that are poorly soluble in water or for electrochemical applications. The present experimental study highlights the specific interest of DES based on decanoic acid (DA) and tetrabutylammonium chloride (TBACl).

Combining experimental approaches, we demonstrate the low polarity of this solvent, that has suitable viscosity, good conductivity and electrochemical property. Moreover, comparing three

different compositions (*n*:*m*), respectively 2:1, 1:1, and 1:2, we reveal the central impact of stoichiometry on these properties. This concerns the thermal stability, that is virtually unlimited for $n \leq m$ due to the suppression of crystallization. Also, an acceleration by two orders of magnitude of the molecular dynamics, as evaluated from the dipolar relaxation and the glass transition, is achieved by increasing the decanoic acid content. This also reflects in different ionic conductivity and electrochemical activity. Finally, the different long-time evolutions of DES after water addition also indicate, at least at a qualitative level, that stoichiometry deeply influences the resistance of DES structure to hydration. Overall, these findings support the interest in DA-TBACl as a solvent with actual potential to fine-tune its properties by varying stoichiometry in order to adapt to specific application requirements.

Declaration of competing interest

The authors declare that they have no known competing financial interests or personal relationships that could have appeared to influence the work reported in this paper.

Acknowledgments

Support from Rennes Metropole and Europe (FEDER Fund – CPER PRINT2TAN) is acknowledged. The authors are grateful to the CNRS – network SolVATE (GDR 2035) for financial support and fruitful discussions

References

1. P. Abbott, A., Capper, G., L. Davies, D., K. Rasheed, R. & Tambyrajah, V. Novel solvent properties of choline chloride/urea mixtures. *Chemical Communications*, 70–71 (2003).
2. Hansen, B. B. *et al.* Deep Eutectic Solvents: A Review of Fundamentals and Applications. *Chem. Rev.* **121**, 1232–1285 (2021).
3. Zhang, Q., Vigier, K. D. O., Royer, S. & Jérôme, F. Deep eutectic solvents: syntheses, properties and applications. *Chem. Soc. Rev.* **41**, 7108–7146 (2012).
4. Dietz, C. H. J. T. *et al.* PC-SAFT modeling of CO2 solubilities in hydrophobic deep eutectic solvents. *Fluid Phase Equilibria* **448**, 94–98 (2017).
5. Florindo, C., Branco, L. C. & Marrucho, I. M. Development of hydrophobic deep eutectic solvents for extraction of pesticides from aqueous environments. *Fluid Phase Equilibria* **448**, 135–142 (2017).
6. Percevault, L., Limanton, E., Nicolas, P., Paquin, L. & Lagrost, C. Electrochemical Determination and Antioxidant Capacity Modulation of Polyphenols in Deep Eutectic Solvents. *ACS Sustainable Chem. Eng.* **9**, 776–784 (2021).
7. Viñas-Ospino, A. *et al.* Comparison of green solvents for the revalorization of orange by-products: Carotenoid extraction and *in vitro* antioxidant activity. *Food Chemistry* **442**, 138530 (2024).
8. Zheng, Q., Yang, F., Tan, H. & Wang, X. Influence of water on the properties of hydrophobic deep eutectic solvent. *The Journal of Chemical Thermodynamics* **195**, 107306 (2024).
9. Martins, M. A. R., Pinho, S. P. & Coutinho, J. A. P. Insights into the Nature of Eutectic and Deep Eutectic Mixtures. *J Solution Chem* **48**, 962–982 (2019).
10. Abbott, A. P. Deep eutectic solvents and their application in electrochemistry. *Current Opinion in Green and Sustainable Chemistry* **36**, 100649 (2022).

11. van Osch, D. J. G. P., Dietz, C. H. J. T., Warrag, S. E. E. & Kroon, M. C. The Curious Case of Hydrophobic Deep Eutectic Solvents: A Story on the Discovery, Design, and Applications. *ACS Sustainable Chem. Eng.* **8**, 10591–10612 (2020).
12. Osch, D. J. G. P. van, Zubeir, L. F., Bruinhorst, A. van den, Rocha, M. A. A. & Kroon, M. C. Hydrophobic deep eutectic solvents as water-immiscible extractants. *Green Chem.* **17**, 4518–4521 (2015).
13. Bahadori, L. *et al.* Physicochemical properties of ammonium-based deep eutectic solvents and their electrochemical evaluation using organometallic reference redox systems. *Electrochimica Acta* **113**, 205–211 (2013).
14. Ruggeri, S. *et al.* Chemical and electrochemical properties of a hydrophobic deep eutectic solvent. *Electrochimica Acta* **295**, 124–129 (2019).
15. Loget, G. *et al.* Direct Electron Transfer of Hemoglobin and Myoglobin at the Bare Glassy Carbon Electrode in an Aqueous BMI.BF4 Ionic-Liquid Mixture. *ChemPhysChem* **12**, 411–418 (2011).
16. D'Hondt, C. & Morineau, D. Dynamics of type V menthol-thymol deep eutectic solvents: Do they reveal non-ideality? *Journal of Molecular Liquids* **365**, 120145 (2022).
17. Hammond, O. S., Bowron, D. T. & Edler, K. J. Liquid structure of the choline chloride-urea deep eutectic solvent (reline) from neutron diffraction and atomistic modelling. *Green Chem.* **18**, 2736–2744 (2016).
18. Kaur, S., Gupta, A. & Kashyap, H. K. Nanoscale Spatial Heterogeneity in Deep Eutectic Solvents. *J. Phys. Chem. B* **120**, 6712–6720 (2016).
19. Posada, E. *et al.* Reline aqueous solutions behaving as liquid mixtures of H-bonded co-solvents: microphase segregation and formation of co-continuous structures as indicated by Brillouin and 1H NMR spectroscopies. *Phys. Chem. Chem. Phys.* **19**, 17103–17110 (2017).

20. Alizadeh, V. *et al.* Strong Microheterogeneity in Novel Deep Eutectic Solvents. *ChemPhysChem* **20**, 1786–1792 (2019).
21. Percevault, L. *et al.* Do Deep Eutectic Solvents Form Uniform Mixtures Beyond Molecular Microheterogeneities? *J. Phys. Chem. B* **124**, 9126–9135 (2020).
22. Kaur, S., Kumari, M. & Kashyap, H. K. Microstructure of Deep Eutectic Solvents: Current Understanding and Challenges. *J. Phys. Chem. B* **124**, 10601–10616 (2020).
23. Reuter, D., Binder, C., Lunkenheimer, P. & Loidl, A. Ionic conductivity of deep eutectic solvents: the role of orientational dynamics and glassy freezing. *Phys. Chem. Chem. Phys.* **21**, 6801–6809 (2019).
24. Jani, A., Malfait, B. & Morineau, D. On the coupling between ionic conduction and dipolar relaxation in deep eutectic solvents: Influence of hydration and glassy dynamics. *The Journal of Chemical Physics* **154**, 164508 (2021).
25. Reuter, D. *et al.* Translational and reorientational dynamics in deep eutectic solvents. *The Journal of Chemical Physics* **154**, 154501 (2021).
26. *Broadband Dielectric Spectroscopy*. (Springer, Berlin, Heidelberg, 2003). doi:10.1007/978-3-642-56120-7.
27. Havriliak, S. & Negami, S. A complex plane analysis of α-dispersions in some polymer systems. *Journal of Polymer Science Part C: Polymer Symposia* **14**, 99–117 (1966).
28. Fröhlich, H. General theory of the static dielectric constant. *Trans. Faraday Soc.* **44**, 238–243 (1948).
29. Díaz-Calleja, R. Comment on the Maximum in the Loss Permittivity for the Havriliak−Negami Equation. *Macromolecules* **33**, 8924–8924 (2000).
30. Böhmer, R., Ngai, K. L., Angell, C. A. & Plazek, D. J. Nonexponential relaxations in strong and fragile glass formers. *The Journal of Chemical Physics* **99**, 4201–4209 (1993).

31. Alvarez, F., Alegra, A. & Colmenero, J. Relationship between the time-domain Kohlrausch-Williams-Watts and frequency-domain Havriliak-Negami relaxation functions. *Phys. Rev. B* **44**, 7306–7312 (1991).
32. Hapiot, P. & Lagrost, C. Electrochemical Reactivity in Room-Temperature Ionic Liquids. *Chem. Rev.* **108**, 2238–2264 (2008).
33. Roldán-Ruiz, M. J., Jiménez-Riobóo, R. J., Gutiérrez, M. C., Ferrer, M. L. & del Monte, F. Brillouin and NMR spectroscopic studies of aqueous dilutions of malicine: Determining the dilution range for transition from a "water-in-DES" system to a "DES-in-water" one. *Journal of Molecular Liquids* **284**, 175–181 (2019).
34. Jani, A., Sohier, T. & Morineau, D. Phase behavior of aqueous solutions of ethaline deep eutectic solvent. *Journal of Molecular Liquids* **304**, 112701 (2020).
35. Malfait, B., Jani, A. & Morineau, D. Confining deep eutectic solvents in nanopores: Insight into thermodynamics and chemical activity. *Journal of Molecular Liquids* **349**, 118488 (2022).